

Membraneless Glucose/O₂ Microfluidic Enzymatic Biofuel Cell using Pyrolyzed Photoresist Film Electrodes

Maria José González-Guerrero^a, Juan Pablo Esquivel^a, David Sánchez-Molas^a, Philippe Godignon^a, Francesc Xavier Muñoz^a, F. Javier del Campo^{*a}, Fabien Giroud^b, Shelley D. Minteer^{*b} and Neus Sabaté^a

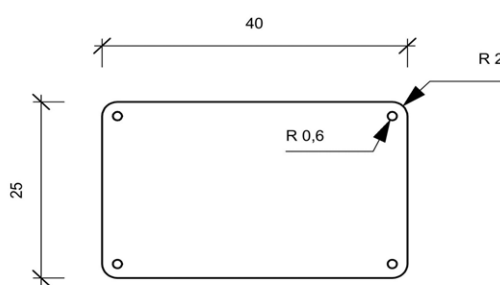
Supplementary Information

This document presents additional information concerning the design of the microfluidic cell described in the manuscript as well as additional results obtained from chips with different electrode separation.

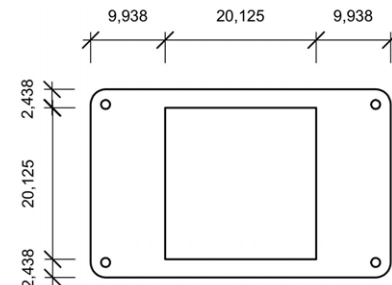
Cell design

The following figures show the design of the microfluidic fuel cell in detail. The units are millimeters. The materials and assembly are described in the manuscript, at *Microfluidic system design and fabrication* section.

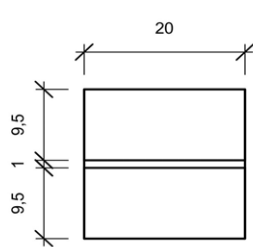
Base layer



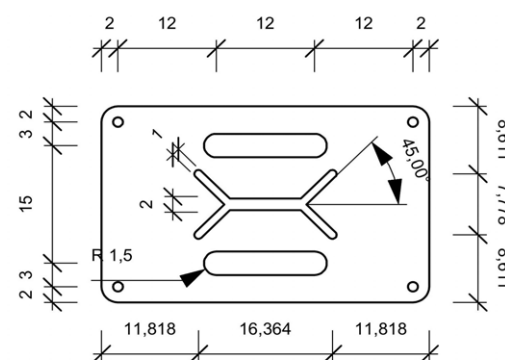
Chip frame

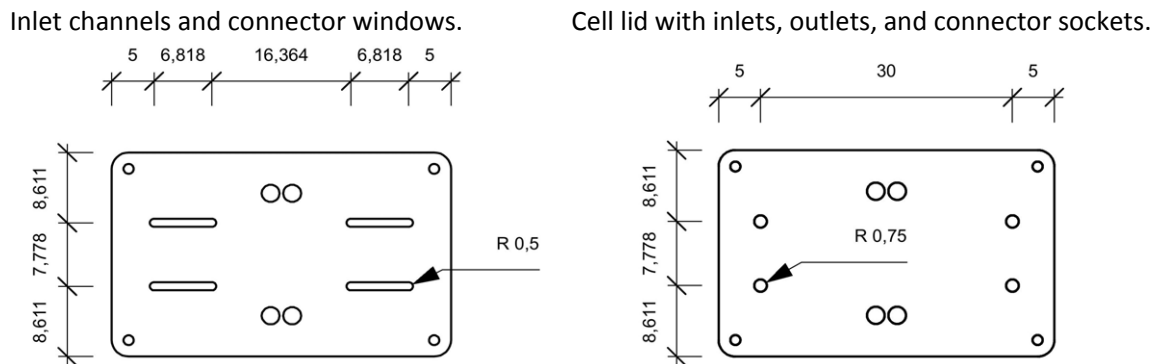


PPF electrodes on silicon – 1mm gap



Double-Y channel centered on top of the electrodes. 2mm wide channel.

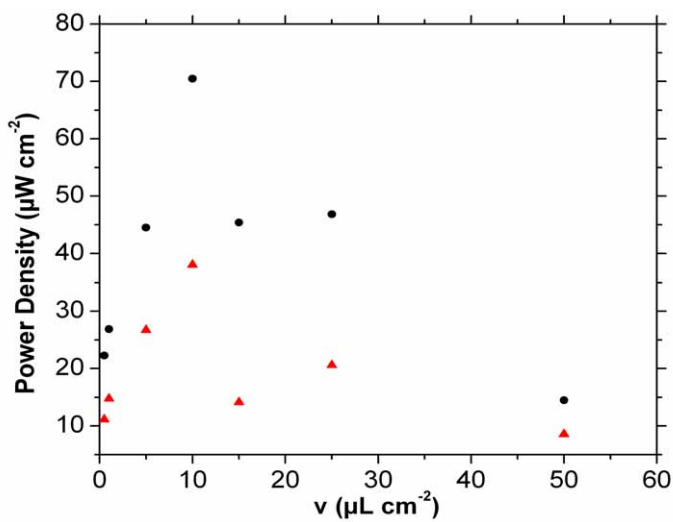




Electrode stability test

Stability tests were performed on a fuel cell with inter-electrode distance of 1mm and a channel width of 2 mm. Before these experiments, the anode and the cathode were tested separately.

To study the time stability of the MBFC, fuel cell performance was measured over a range of flow-rates. Then, the cell was dried and stored at 4°C in a refrigerator for 24 hours. After this, the measurements were repeated. Figure SF1 displays typical power densities as a function of flow rate recorded in one of these experiments, showing that the best performance was obtained at a flow rate of 10 $\mu\text{L min}^{-1}$. Although we appreciate similar trends in both curves, after 24 hours of storage at 4°C, we found the output power dramatically diminishes almost down to 50 % of the original power value. This relatively poor stability of the modified electrodes was attributed to the loss of enzyme activity caused by the non-covalent attachment of the enzymes to the electrodes, and to the drying of the electrodes prior to storage.



SF1. Power density as a function of flow rate. In red, stability of the enzymatic microfluidic fuel cell after 24 hours of storage at 4°C. The power of density was calculated from the nominal active area of the electrode.

Fuel cell performance vs. Flow rate.

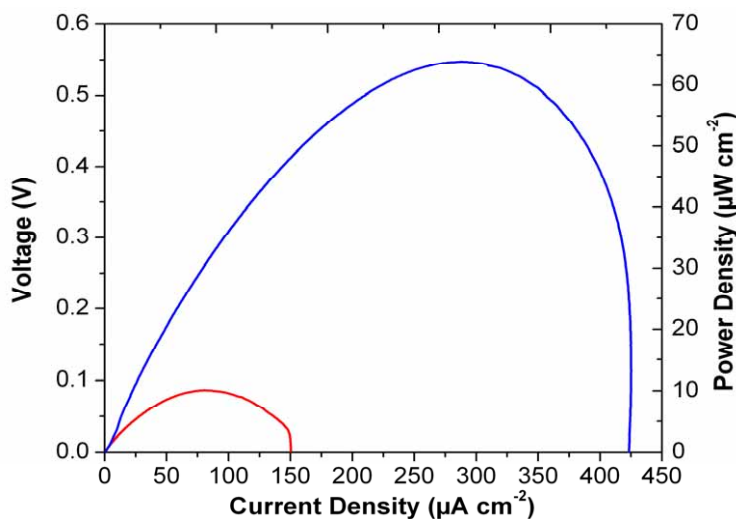
The following data corresponds to figure 3 in the manuscript, and are the result of three replicate experiments.

Table ST1. Figures of merit of each curve used for the construction of the maximum biofuel cell power output as a function of flow rate (Figure 3).

v ($\mu\text{L min}^{-1}$)	V_{\max} (V)	P_{\max} ($\mu\text{W cm}^{-2}$)	j at P_{\max} ($\mu\text{A cm}^{-2}$)
1	0.51 (± 0.01)	11.9 (± 2.3)	54.3 (± 8.8)
10	0.57 (± 0.02)	27.3 (± 3.7)	121.0 (± 14.0)
20	0.56 (± 0.02)	40.1 (± 5.2)	170.7 (± 18.5)
30	0.54 (± 0.04)	51.2 (± 5.8)	205.6 (± 22.4)
40	0.55 (± 0.03)	60.1 (± 5.6)	263.6 (± 25.7)
50	0.52 (± 0.05)	62.1 (± 6.3)	272.3 (± 26.0)
60	0.50 (± 0.04)	61.3 (± 5.9)	275.4 (± 27.2)
70	0.54 (± 0.04)	63.8 (± 5.2)	290.2 (± 28.3)
80	0.49 (± 0.05)	63.2 (± 6.7)	279.7 (± 25.8)

Typical fuel cell power output curves.

In addition to Figure 4 in the manuscript (Polarization and power curve obtained from the glucose microfluidic biofuel cell), figure SF2 shows the power density curves with and without glucose.



SF2. Polarization curves obtained for the biofuel cell at $70 \mu\text{L min}^{-1}$, with (blue) and without (red) glucose.